Discovery of Diazepane Amide DORAs and 2-SORAs Enabled by Exploration of Isosteric Quinazoline Replacements

Anthony J. Roecker, Swati P. Mercer, Jeffrey M. Bergman, Kevin F. Gilbert, Scott D. Kuduk, C. Meacham Harrell, Susan L. Garson, Steven V. Fox, Anthony L. Gotter, Pamela L. Tannenbaum, Thomayant Prueksaritanont, Tamara D. Cabalu, Donghui Cui, Wei Lemaire, Christopher J. Winrow, John J. Renger, Paul J. Coleman

PII: S0960-894X(14)01389-4
DOI: http://dx.doi.org/10.1016/j.bmcl.2014.12.081
Reference: BMCL 22326

To appear in: *Bioorganic & Medicinal Chemistry Letters*

Received Date: 27 November 2014
Revised Date: 22 December 2014
Accepted Date: 24 December 2014

Please cite this article as: Roecker, A.J., Mercer, S.P., Bergman, J.M., Gilbert, K.F., Kuduk, S.D., Meacham Harrell, C., Garson, S.L., Fox, S.V., Gotter, A.L., Tannenbaum, P.L., Prueksaritanont, T., Cabalu, T.D., Cui, D., Lemaire, W., Winrow, C.J., Renger, J.J., Coleman, P.J., Discovery of Diazepane Amide DORAs and 2-SORAs Enabled by Exploration of Isosteric Quinazoline Replacements, *Bioorganic & Medicinal Chemistry Letters* (2015), doi: http://dx.doi.org/10.1016/j.bmcl.2014.12.081

Discovery of Diazepane Amide DORAs and 2-SORAs Enabled by Exploration of Isosteric Quinazoline Replacements

Anthony J. Roecker,*[,a] Swati P. Mercer,[a] Jeffrey M. Bergman,[a] Kevin F. Gilbert,[a] Scott D. Kuduk,[a] C. Meacham Harrell,[b] Susan L. Garson,[b] Steven V. Fox,[b] Anthony L. Gotter, [b] Pamela L. Tannenbaum,[b] Thomayant Prueksaritanont,[c] Tamara D. Cabalu,[c] Donghui Cui,[c] Wei Lemaire,[d] Christopher J. Winrow,[b] John J. Renger,[b] and Paul J. Coleman[a]

Departments of Medicinal Chemistry,[a] Neuroscience,[b] Drug Metabolism,[c] and In Vitro Pharmacology,[d] Merck Research Laboratories, P. O. Box 4, Sumneytown Pike, West Point, PA 19486.

* Corresponding author. Tel.: + 1-215-652-8257; fax: + 1-215-652-3971; e-mail: anthony_roecker@merck.com

Abstract

Dual orexin receptor antagonists (DORAs), or orexin 1 (OX_1) and orexin 2 (OX_2) receptor antagonists, have demonstrated clinical utility for the treatment of insomnia. Medicinal chemistry efforts focused on the reduction of bioactivation potential of diazepane amide **1** through the modification of the Western heterocycle resulted in the discovery of suvorexant, a DORA recently approved by the FDA for the treatment of insomnia. A second strategy towards reducing bioactivation risk is presented herein through the exploration of monocyclic quinazoline isosteres, namely substituted pyrimidines. These studies afforded potent DORAs with significantly reduced bioactivation risk and efficacy in rodent sleep models. Surprisingly, side products from the chemistry used to produce these DORAs yielded isomeric pyrimidine-containing diazepane amides possessing selective OX_2R antagonist (2-SORA) profiles. Additional exploration of these isomeric pyrmidines uncovered potent 2-SORA diazepane amides with sleep efficacy in mouse EEG studies.

Results and Discussion

The field of orexin receptor antagonist research began shortly after the discovery of the orexin receptors, OX_1R and OX_2R, and their wake-promoting peptides, orexin A and B, in 1998.[1] Proof-of-concept for the treatment of insomnia by dual orexin receptor antagonists (DORAs, molecules that antagonize both receptors) occurred in under a decade in 2007,[2] and suvorexant (**2**, Figure 1) was the first DORA to be approved by the FDA for the treatment of insomnia in 2014.[3] Several excellent reviews describing the state of preclinical and clinical orexin antagonist research have been published and are beyond the scope of this manuscript.[4] Medicinal chemistry efforts that resulted in the discovery of suvorexant have been published by our group.[5] The reduction of bioactivation potential was a critical profile element in the optimization of diazepanes such as **1**[6] to suvorexant (**2**).[7] Metabolite identification studies revealed the fluoroquinazoline motif in **1** was the underlying cause of the bioactivation through the formation of high levels of GSH adducts in human and rat microsomal incubations. Suvorexant demonstrated that modification of the nature of the fused Western heterocycle could significantly reduce bioactivation potential in the same microsomal GSH trapping experiments. A second strategy targeted utilization of monocyclic isosteric replacements (**3**, Figure 1) of the fluoroquinazoline heterocycle in **1** to affect a similar level of bioactivation risk reduction.

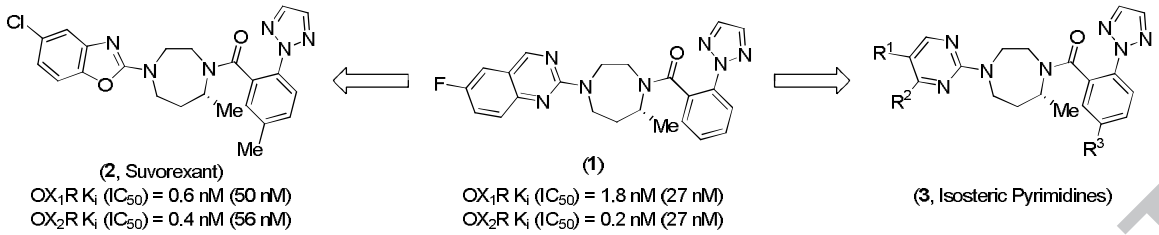

Figure 1. Strategic designs focused on reduction of bioactivation potential of diazepane amide DORA **1**.

Analysis of previously disclosed SAR in the diazepane amide DORA series demonstrated that removal of the distal fused phenyl in the Western heterocycle afforded essentially inactive compounds at both receptors (data not shown).[8] From this data it was apparent that the lipophilic interactions in this region of the molecule were critical from a potency perspective. Thus, substituted pyrimidine Western heterocyclic designs filling a similar amount of lipophilic space compared to DORA **1** were prioritized for synthetic efforts. The synthesis of selected targets is described in Schemes 1 and 2. Substitution reactions involving diazepane cores **A** and **B** with 5-substituted-2,4-dichloropyrimidines favor substitution at the 4-position of the pyrimidine except when a strong electron withdrawing motif is present at the 5-position.[9] An example of reversed regioselectivity in these S_NAr reactions is depicted in Scheme 1 as diazepane amines **A** and **B** react with 2,4-dichloro-5-trifluoromethylpyrimidine (**C**) to afford the 2-substituted products **7** and **8** in a 4:1 ratio with regioisomers **13** and **14**.[10] Both regioisomeric products were then transformed via a second S_NAr reaction or Stille coupling to afford products **9** - **12** and **15** in acceptable yields. The regioselectivity for the initial S_NAr reaction was confirmed by small molecule X-ray analysis of DORA **11** (Scheme 1). A more standard selectivity profile for these S_NAr reactions is depicted in Scheme 2 where 2,4,5-trichloropyrimidine (**F**) must be functionalized via selective Stille coupling with tetramethyltin to afford

intermediate **G**.[11] This intermediate can then be reacted with diazepane core **A** to afford 2-substituted pyrimidine compound **4** in high yield. The substitution reaction of **F** with diazepane core **B** was completely selective for the 4-position of the pyrimidine to afford **18**. Compound **18** was then regioselectively methylated under Stille conditions to afford compound **19**.

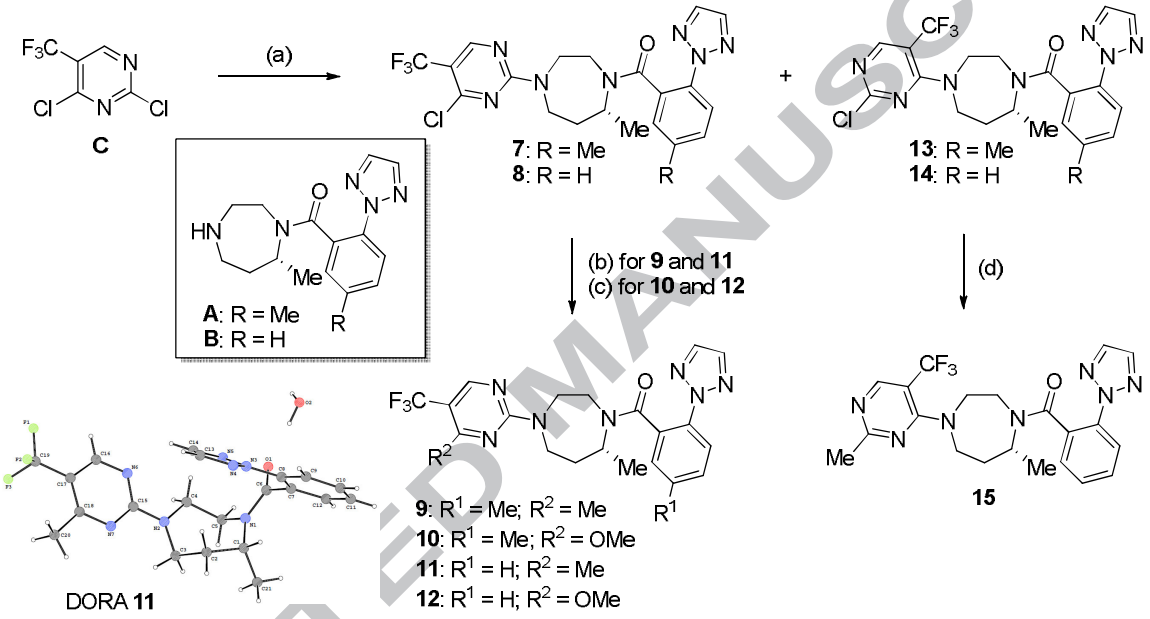

Scheme 1. Representative synthesis of diazepane amide DORAs. Reagents and reaction conditions: (a) Diazepane **A**, Et_3N, DMF, 25°C, 18h, 67% of **7** and 18% of **13**; Diazepane **B** afforded 56% of **8** and 16% of **14**; (b) Me_4Sn, $PdCl_2$(dppf), LiCl, DMF, 110°C, 14h, 70% for **9** 86% for **11**; (c) NaOMe (4M in MeOH), DMF, 23°C, 0.5h, 95% for **10** and 96% for **12**; (d) Me_4Sn, $PdCl_2$(dppf), LiCl, DMF, 110°C, 14h, 19%; See reference 5a for the synthesis of diazepane cores **A** and **B**; Abbreviations: DMF = N,N-dimethylformamide, dppf = 1,1'-(diphenylphosphino)ferrocene.

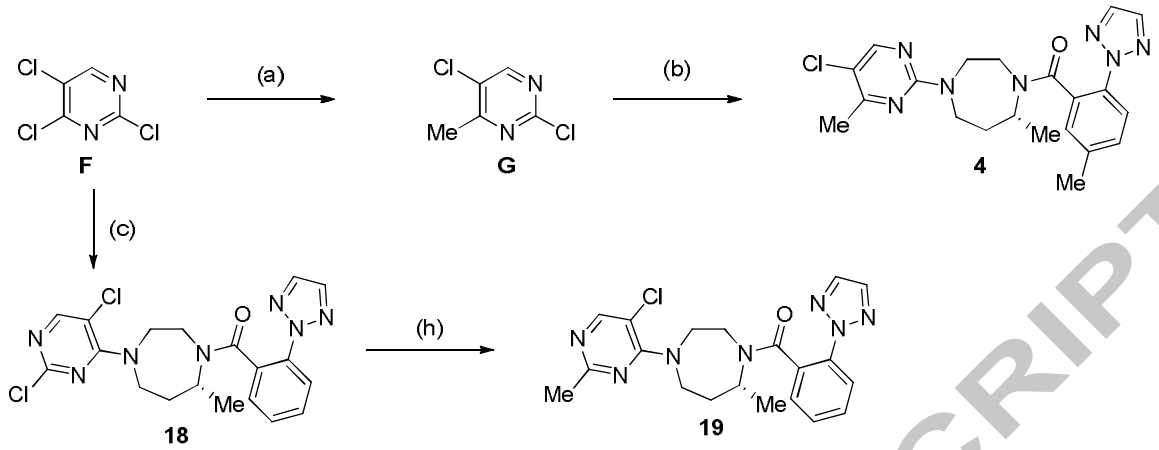

Scheme 2. Representative synthesis of diazepane amide DORAs and 2-SORAs. Reagents and reaction conditions: (a) Me_4Sn, $PdCl_2(dppf)$, DMF, 110°C, 4h, 60%; (b) Diazepane **A**, Et_3N, DMF, 90°C, 15h, 56%; (c) Diazepane **B**, Et_3N, DMF, 0°C to 23°C, 18h, 73%; (d) Me_4Sn (1.05 equiv), $Pd(PPh_3)_4$, LiCl, DMF, 115°C, 4h, 43%

Selected potency and pharmacokinetic data for isosteric replacements of the Western 6-fluoroquinazoline motif are captured in Table 1. While certain designs did not recapitulate the planar topology of the fused fluorophenyl ring of DORA **1** (i.e. compounds **7 – 12** containing a trifluoromethyl motif), all designs resided within 20 $Å^2$ of lipophilic surface area from the lead.[12] As shown in Table 1, compound **1** demonstrated excellent binding (as determined by a radioligand binding assay) and functional (as determined via FLIPR assay) potency at OX_2R and OX_1R as well as low clearance in the dog.[13] This combination of potency and pharmacokinetics provided excellent sleep efficacy in preclinical models and eventually led to the discovery of suvorexant (**2**). Hence, our objective was to duplicate this excellent profile in a monocyclic pyrimidine DORA.

Replacement of the fluorophenyl motif in DORA **1** with chlorine and methyl substituents such as **4** and **5** retained excellent binding and functional potency of lead **1** on both receptors. However, clearance in dog increased 3-fold for both compounds. Concerns around the direct electrophilic potential of the 4-chloropyrimidine motif in

DORA **5** encouraged non-electrophilic designs such as 4-methoxy-5-methylpyrimidine **6**. OX_1R binding potency and functional potency on both receptors were slightly diminished for this analog. Analogs such as **7** were designed incorporating a 5-trifluoromethyl motif to interrogate the relationship between lipophilicity and potency. Gratifyingly, compound **7** demonstrated subnanomolar intrinsic potency against OX_2R and OX_1R, however, functional potency significantly diminished and dog clearance increased with the incorporation of lipophilicity. Reducing lipophilicity via removal of the methyl group (**8**, Table 1) on the triazole benzamide did not further improve functional potency, and, coupled with concerns around direct electrophilicity of compounds **7** and **8**, chlorine replacements were targeted. Analogs **9** through **12** replaced the potentially electophilic chlorine in compounds **7** and **8** with a methyl or methoxy motif. Both compounds **9** and **10** demonstrated excellent intrinsic potency against both receptors, however, the methoxy analog **10** displayed improved functional potency and reduced clearance in dog compared to compound **9**. Removing the methyl group from the triazole benzamide afforded **11** and **12** with very comparable functional potency and dog clearance profiles compared to DORA **10**. Consistent with known amide SAR in the diazepane series, compounds **11** and **12** demonstrated reduced OX_1R binding potency. Hence, the profile of DORA **10** most closely replicated the potency and pharmacokinetic profile of DORA **1**, and this compound was selected for additional profiling.

Table 1. Potential quinazoline isosteric replacements.[a,b]

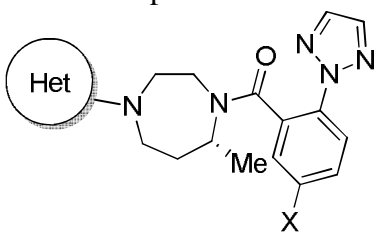

Heterocycle (compound #)	X	OX_2R K_i (nM)[a]	OX_1R K_i (nM)[a]	OX_2R IC_{50} (nM)[a]	OX_1R IC_{50} (nM)[a]	Dog Cl (mL/min/kg)
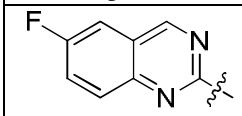 (**1**)	H	0.2	1.8	27	27	3
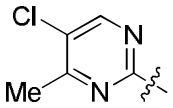 (**4**)	Me	0.6	6.1	20	26	9
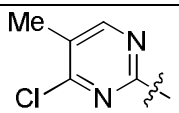 (**5**)	Me	0.4	3.9	28	30	8
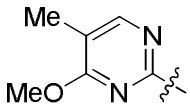 (**6**)	Me	0.6	14	31	38	NA
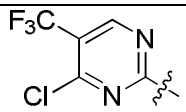 (**7**)	Me	0.6	0.7	140	120	15
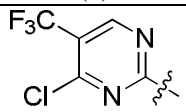 (**8**)	H	0.7	5.1	88	99	NA
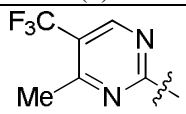 (**9**)	Me	0.5	1.6	85	52	10
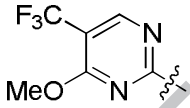 (**10**)	Me	0.4	1.5	27	43	3
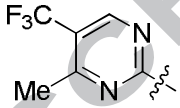 (**11**)	H	0.5	11	19	27	5
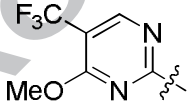 (**12**)	H	0.7	6.3	21	44	3

(a) See reference 5a for the details of these assays. All compounds listed were assayed as single enantiomers; (b) All data reported as an average value from $n \geq 2$; for $n > 2$, standard deviation is < 40% in all cases.

The bioactivation potential of DORA **1** and DORA **10** was assessed *in vitro* through glutathione (GSH) trapping experiments in rat and human microsomal preparations. DORA **10** reduced the amount of GSH-related adducts (determined by AUC measurements normalized to an internal standard) compared to DORA **1** in both rat and human preparations by over 80% (Figure 2).[14] This reduction in bioactivation potential was comparable to that achieved by the chloro-benzoxazole motif in suvorexant (>95% reduction, **2**, Figure 1). DORA **10** demonstrated similar plasma protein binding in rat and human (95% and 96%, respectively), however, it was highly bound in dog (99.5%). The compound was highly permeable, was not a substrate for rat or human Pgp,[15] and it owned moderate PSA and relatively high lipophilicity (logD = 3.4) suggesting high potential for CNS penetration (Figure 3). DORA **10** has moderate clearance in rat and low clearance in dog with short half-lives in both species consistent with a short-acting agent for insomnia treatment (Table 2). Although DORA **10** had limited bioavailability in rat (8%), it demonstrated moderate bioavailability in the dog (23%). With this information in hand, increased doses were targeted in rat sleep experiments to evaluate oral efficacy of DORA **10** compared to lead DORA **1**.

Figure 2. GSH trapping studies of DORAs **1** and **10** in rat and human liver microsomes.[a]

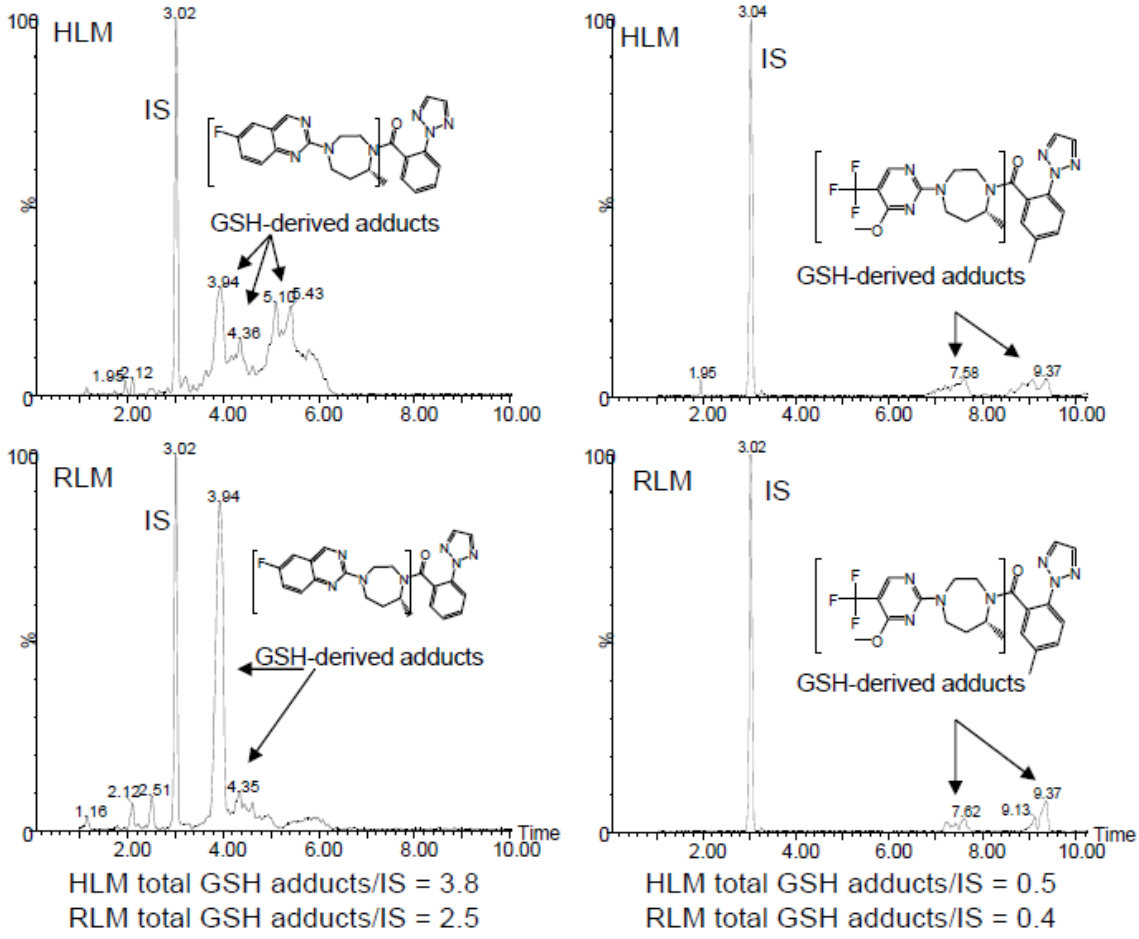

[a] Ratios are AUC measurements normalized to the AUC of an internal standard (IS = labetalol). AUC = area under curve; RLM = rat liver microsomes; HLM = human liver microsomes.

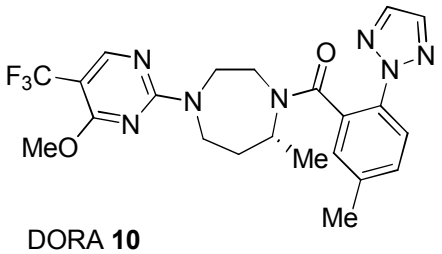

DORA **10**

Plasma Protein Binding
Human: 96%
Rat: 95%
Dog: 99.5%

CNS Properties
Pgp ratio (BA/AB): 0.7 (h); 1.2 (r)
Papp: 28 cm * 10^{-6}/s
HPLC log D: 3.4
PSA: 78 Å^2
MW: 475 g/mol

Figure 3. Additional properties of DORA **10**.

Table 2. Pharmacokinetics of DORA **10** in rat and dog.

	IV[a]					PO[b]			
Species	Dose (mg/kg)	Cl (mL/min/kg)	Vd_{ss} (L/kg)	$T_{1/2}$ (h)	Dose (mg/kg)	AUC (μM*h)	T_{max} (h)	C_{max} (μM)	F (%)
Rat	2	37	2.5	1.1	10	0.6	3.0	0.2	8
Dog	0.125	3	0.4	2.4	3[c]	9.9	0.6	2.3	23
Rat	NA	NA	NA	NA	30[c]	5.5	0.8	2.5	19

[a] vehicle = 100% DMSO in rat and dog (n = 2); [b] dosed as the free base in 100% PEG200 (n = 2); [c] dosed as free base in 20% VitE TPGS in water; satellite rats for sleep study pharmacokinetics (n = 3), PO in dog n = 2.

Figure 4. Sleep architecture effects of DORA **10** and DORA **1** in rat sleep dosed during their active phase.[a]

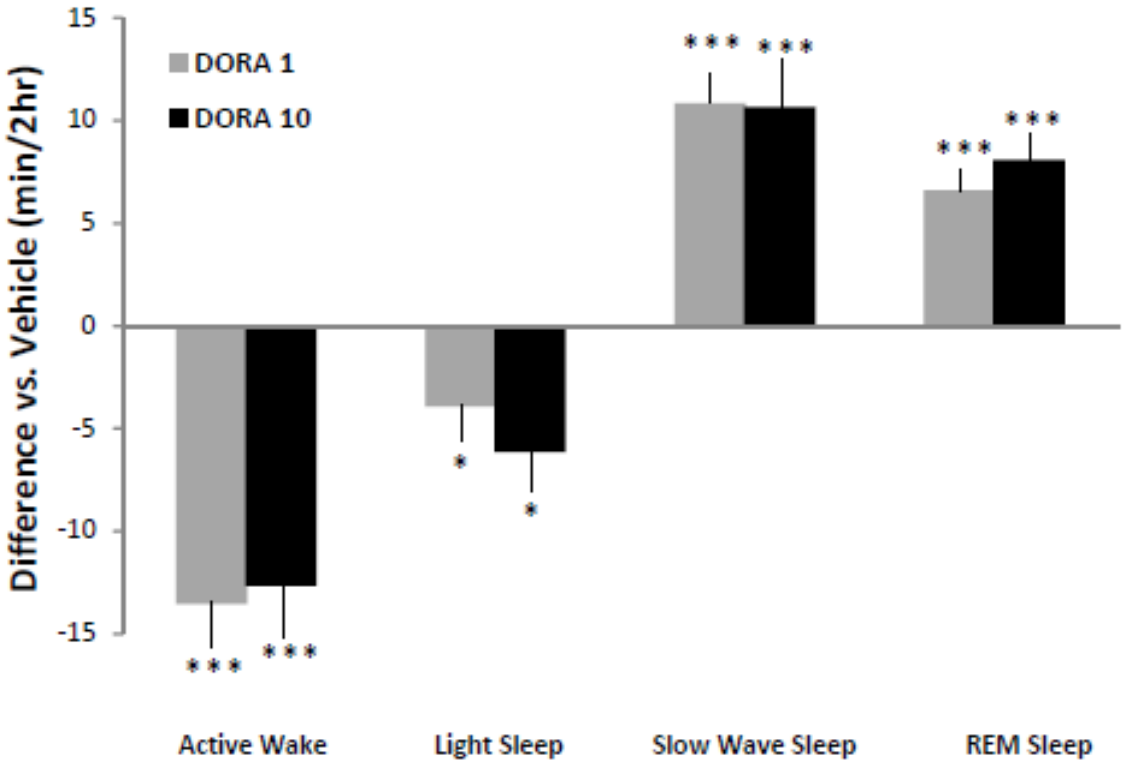

Mean time in active wake, light sleep, SWS and REM sleep in rat monitored for two hours post dose. PO administration of 30mg/kg of DORA **1**, 30 mg/kg of DORA **10**, or vehicle (20% Vitamin E TPGS) treatment was administered in a balanced cross-over design such that each subject received drug and vehicle (3 day treatment). Mean within-subject change relative to vehicle is shown. Data were analyzed using within-subject ANOVA to determine main effects and one sample t-test to compare to vehicle (N = 12); (*$p < 0.05$, **$p < 0.01$, ***$p < 0.001$).

Comparative efficacy for DORAs **1** and **10** in our previously reported rat sleep model is depicted in Figure 4.[16] Immediate, significant, and statistically similar reductions of active wake and concomitant increases in slow wave and REM sleep were observed for both compounds during the first two hours after oral administration of 30 mpk of each DORA (active-phase dosing). Pharmacokinetics in satellite rats determined that DORA **10** achieved significant exposure in the sleep experiment with a C_{max} of 2.5 µM, an AUC of 5.5 µM•h, and a T_{max} of 0.8 h. These exposure levels indicate significant OX_2R occupancy during the course of the experiment as DORA **10** achieved 83% occupancy in a humanized rat occupancy model at a plasma exposure of 1.0 µM.[17] The

exposure / occupancy relationship for lead DORA **1** was very similar to that described above with C_{max} of 2.0 μM, an AUC of 4.5 μM•h in rat sleep studies, a T_{max} of 1.3 h, and 90% occupancy at 0.35 μM. Hence, from a potency, pharmacokinetic, and efficacy perspective, the 4-methoxy-5-trifluoromethylpyrimidine motif was a competent isosteric replacement for 6-fluoroquinazoline substructure with the potential to significantly reduce bioactivation potential.

In addition to assaying the purposefully designed isosteric replacements of DORA **1**, our team also studied the regioisomeric S_NAr products from Scheme 1. Previous SAR as well as SAR established in Table 1 (see matched pairs **9** and **11**; **10** and **12**, Table 1) demonstrated that the removal of the methyl group on the benzamide of suvorexant (**2**, Figure 1) generally resulted in the reduction of OX_1R binding and, in some cases, functional potency. Hence, it was expected that compounds such as **14** would demonstrate some level of reduced OX_1R potency. Surprisingly, compound **14** had significantly diminished OX_1R binding potency (K_i = 1100 nM, Table 3) and was essentially functionally inactive on OX_1R. Compound **14** displayed moderate binding and functional potency on OX_2R which established this compound as a selective orexin 2 receptor antagonist (2-SORA) lead with selectivity over OX_1R of greater than 139-fold. 2-SORAs have recently been of interest to further delineate receptor specific pharmacology as well as therapeutic entities themselves.[18] The 2-chloropyrimidine motif embedded in compound **14** was a concern due to innate electrophilicity similar to the DORA effort above, thus a small SAR effort was undertaken to remove this concern and improve OX_2R potency.

Replacement of the 2-chloropyrimidine with a 2-methylpyrimidine to remove the nascent electophilic potential of **14** afforded 2-SORA **15** with diminished both OX_2R binding and functional potency.[19] Replacement of the trifluoromethyl motif of **14** with a methyl group increased OX_2R potency in both matched pairs (**14** and **16**; **15** and **17**), however, 2-SORA **17** still was not in an OX_2R potency range comparable to DORA **1** and suvorexant (**2**, Figure 1). Further modifying the 5-substituent of the pyrimidine to a chlorine gave a marked OX_2R potency increase for both **18** and **19**, and 2-SORA **19** possessed OX_2R functional potency (48 nM) similar to suvorexant (56 nM) with no detectable antagonist activity on OX_1R (> 200x selectivity). Due to its lack of potentially overt electrophilicity and favorable potency and selectivity profile, 2-SORA **19** was selected for additional profiling.

Table 3. Regioisomeric pyrimidines with 2-SORA profiles.[a,b]

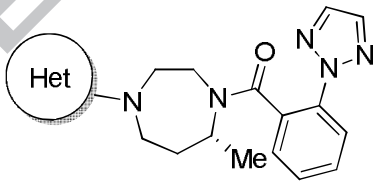

Heterocycle (compound #)	OX_2R K_i (nM)[a]	OX_1R K_i (nM)[a]	OX_2R IC_{50} (nM)[a]	OX_1R IC_{50} (nM)[a]	Selectivity (OX_1R IC_{50} / OX_2R IC_{50})
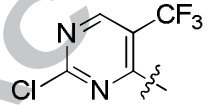 (**14**)	7.7	1100	72	>10000	> 139
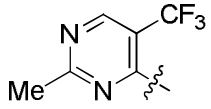 (**15**)	31	4200	88	>10000	> 114

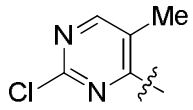 (**16**)	2.6	760	42	2600	62
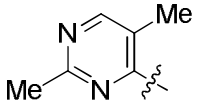 (**17**)	12	3600	82	>10000	> 122
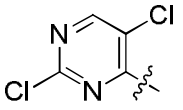 (**18**)	1.1	850	25	3200	128
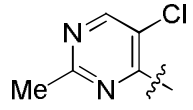 (**19**)	3.6	1800	48	>10000	> 208

(a) See reference 5a for the details of these assays. All compounds listed were assayed as single enantiomers; (b) All data reported as an average value from n ≥ 2; for n > 2, standard deviation is < 40% in all cases.

2-SORA **19** displayed properties consistent with CNS penetration such as high permeability, low molecular weight, moderate PSA, and moderate log D (Figure 5). This compound was not a substrate for rat or human Pgp and possessed acceptable free fraction across species. Pharmacokinetic evaluation of 2-SORA **19** indicated moderate clearance in dog and high clearance in rat with short half-lives in both species (Table 4). Despite high clearance, the compound demonstrated moderate bioavailability in both rat (%F = 35%) and dog (%F = 19) suggesting that evaluation of oral sleep efficacy would be possible. Due to high clearance in rat for 2-SORA **19**, high doses for in vivo evaluation were anticipated. Thus, mouse sleep studies were selected to probe efficacy for this 2-SORA lead to ease material requirements, and active-phase oral dosing at 300 mpk to telemetrized mice elicited immediate and significant decreases in active wake with concomitant increases in delta and REM sleep over the course of two hours (Figure 6). While exposures were somewhat high in this experiment (C_{max} = 18 μM),[20] these findings

are very consistent with sleep architecture profiles for DORA **10**, DORA **1**, suvorexant, and 2-SORAs MK-1064 and MK-3697.[21]

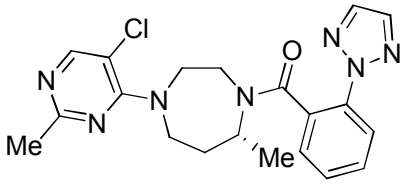

2-SORA **19**

Plasma Protein Binding
Human: 95%
Rat: 88%
Dog: 95%

CNS Properties
Pgp ratio (BA/AB): 0.7 (h); 1.5 (r)
Papp: 34 cm * 10^{-6}/s
HPLC log D: 2.8
PSA: 74 $Å^2$
MW: 412 g/mol

Figure 5. Additional properties of 2-SORA **19**.

Table 4. Pharmacokinetics of 2-SORA **19** in rat and dog.

	IV[a]					PO[b]			
Species	Dose (mg/kg)	Cl (mL/min/kg)	Vd_{ss} (L/kg)	$T_{1/2}$ (h)	Dose (mg/kg)	AUC (μM*h)	T_{max} (h)	C_{max} (μM)	F (%)
Rat	2	118	7.0	3.2	10	1.2	0.4	0.9	35
Dog	0.5	15	0.8	0.9	3[c]	1.8	0.4	1.3	19
Mouse[c]	NA	NA	NA	NA	300	NA	1.0	18	NA

[a] vehicle = 100% DMSO in rat and dog (n = 2); [b] dosed as the hydrochloride salt in 100% PEG200 (n = 2); [c] dosed as free base in 20% VitE TPGS in water; satellite rats for sleep study pharmacokinetics (n = 3), PO in dog n = 2.

Figure 6. Sleep architecture effects of 2-SORA **19** in mouse sleep experiments dosed during their active phase.[a]

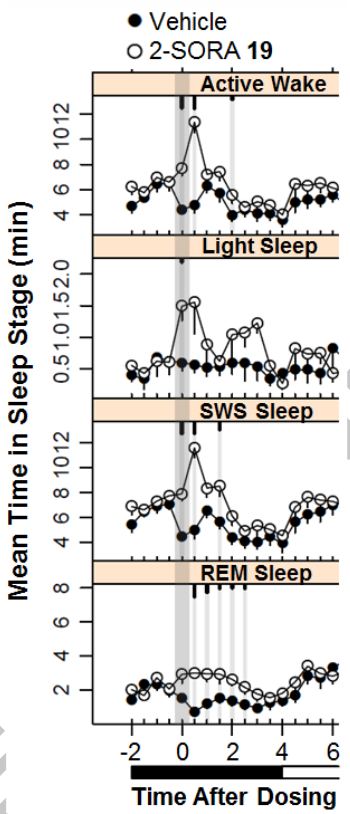

Mean time in active wake, light sleep, SWS and REM sleep in wild type mice monitored for over time. PO administration of 2-SORA **19** (300 mg/kg; open circles) or vehicle (closed circles; 20% Vitamin E TPGS) treatment was administered in a balanced cross-over design such that each subject received drug and vehicle (5 day treatment). Vertical grey bar indicates dose time relative to light/dark period (filled/open horizontal bar). Significant differences are indicated by gray vertical lines, and black tic marks indicate significance level (short, medium, long, $p < 0.05$, 0.01, 0.001).

In conclusion, we have demonstrated that substituted pyrimidines can serve as competent isosteric replacements for the 6-fluoroquinzaoline motif with the added benefit of lower bioactivation potential with DORA **10** representing a hallmark example. During the course of synthesis, we serendipitously discovered that isomeric pyrimidines in the diazepane amide series owned moderate OX_2R potency and significant selectivity over OX_1R making them intriguing 2-SORA leads. Further exploration uncovered 2-SORA **19**

as an orally efficacious 2-SORA in mouse sleep. Further biological studies on DORAs and 2-SORAs presented herein will be published in due course.

Acknowledgments

We thank Dr. Charles W. Ross III and Joan S. Murphy for analytical studies in support of this manuscript. We would like to thank Michael J. Bogusky for NMR support. We would like to thank Joseph G. Bruno and Rodney A. Bednar for assay support.

[1] a) L. De Lecea, T. S. Kilduff, C. Peyron, X.-B. Gao, P. E. Foye, P. E. Danielson, C. Fukuhara, E. L. F. Battenberg, V. T. Gautvik, F. S. Bartlett II, W. N. Frankel, A. N. Van Den Pol, F. E. Bloom, K. M. Gautvik, and J. G. Sutcliffe, *Proc. Natl. Acad. Sci. USA* **1998**, *95*, 322 – 327; b) T. Sakurai, A. Amemiya, M. Ishii, I. Matsuzaki, R. Chemelli, H. Tanaka, S. C. Williams, J. A. Richardson, G. P. Kozlowski, S. Wilson, J. R. S. Arch, R. E. Buckingham, A. C. Haynes, S. A. Carr, R. S. Annan, D. E. McNulty, W. Liu, J. A. Terrett, N. A. Elshourbagy, D. J. Bergsma, M. Yanagisawa, *Cell* **1998**, *92*, 573 – 585.

[2] a) C. Brisbare-Roch, J. Dingemanse, R. Koberstein, P. Hoever, H. Aissaoui, S. Flores, C. Mueller, O. Nayler, J. van Gerven, S. L. de Haas, P. Hess, C. Qiu, S. Buchmann, M. Scherz, T. Weller, W. Fischli, M. Clozel, F. Jenck, *Nature Medicine* **2007**, *13*, 150 – 155; b) P. Hoever, G. Dorffner, H. Benes, T. Penzel, H. Danker-Hopfe, M. J. Barbanoj, G. Pillar, B. Saletu, O. Polo, D. Kunz, J. Zeitlhofer, S. Berg, M. Partinen, C. L. Bassetti, B. Hogl, I. O. Ebrahim, E. Holsboer-Traschsler, H. Bengtsson, Y. Peker, U.-M. Hemmeter, E. Chiossi, G. Hajak, J. Dingemanse, *Clin. Pharmacol. Ther.* **2012**, *91*, 975-985.

[3] Suvorexant (Belsomra®) was approved by the FDA for the treatment of insomnia on August 13, 2014; see http://www.fda.gov/NewsEvents/Newsroom/PressAnnouncements/ucm409950.htm

[4] For recent reviews focused on orexin medicinal chemistry and biology, see: (a) Gotter, A. L.; Webber, A. L.; Coleman, P. J.; Renger, J. J.; Winrow, C. J. International Union of Basic and Clinical Pharmacology. LXXXVI. *Pharmacological Reviews* **2012**, *64*, 389-420; (b) Gotter, A. L.; Roecker, A. J.; Hargreaves, R.; Coleman, P. J.; Winrow, C. J.; Renger, J. J. *Progr. Brain Res.* **2012**, *198*, 163-188; (c) Scammell, T. E. and Winrow, C. J. *Annu. Rev. Pharmacol. Toxicol.* **2011**, *51*, 243-266; (d) Sakurai, T.; Mieda, M. *Trends Pharmacol. Sci.* **2011**, *32*, 451-462; (e) Ruoff, C.; Cao, M.; Guilleminault, C. *Curr. Pharm. Des.* **2011**, *17*, 1476-1482; (f) Carter, M. E.; Borg, J. S.; de Lecea, L. *Curr. Opin. Pharmacol.* **2009**, *9*, 39-45; (g) Chiou, L.-C.; Lee, H.-J.; Ho, Y.-C.; Chen, S.-P.; Liao, Y.-Y.; Ma, C.-H.; Fan, P.-C.; Fuh, J.-L.; Wang, S.-J. *Curr. Pharm. Des.* **2010**, *16*, 3089-3100; (h) Cao, M.; Guilleminault, C. *Curr. Neurol. Neurosci. Rep.* **2011**, *11*, 227-234; (i) Winrow, C. J.; Renger, J. J. *Br. J. Pharmacol.* **2014**, *171*, 283-293; (j) Kuduk, S. D.; Winrow, C. J.; Coleman, P. J. *Ann. Rep. Med. Chem.* **2013**, *48*, 73-87; (k) Gatfield, J.; Brisbare-Roch, C.; Jenck, F.; Boss, C. *ChemMedChem* **2010**, *20*, 1539-1542.

[5] (a) Cox, C. D.; Breslin, M. J.; McGaughey, G. B.; Whitman, D. B.; Schreier, J. D.; Bogusky, M. J.; Roecker, A. J.; Mercer, S. P.; Bednar, R. A.; Lemaire, W.; Bruno, J. G.; Reiss, D. R.; Harrell, C. M.; Murphy, K. L.; Garson, S. L.; Doran, S. M.; Koblan, K. S.; Prueksaritanont, T.; Anderson, W. B.; Tang, C.; Roller, S.; Cabalu, T. D.; Cui, D.; Ball, R. G.; Hartman, G. D.; Winrow, C. J.; Renger, J. J.; Coleman, P. J. *J. Med. Chem.* **2010**, *53*, 5320 – 5332; (b) Winrow, C. J.; Gotter, A. L.; Cox, C. D.; Doran, S. M.;

Tannenbaum, P. L.; Breslin, M. J.; Garson, S. L.; Fox, S. V.; Harrell, C. M.; Stevens, J.; Reiss, D. R.; Cui, D.; Coleman, P. J.; Renger, J. J. *J. Neurogenetics* **2011**, *25*, 52-61.

[6] Compound **1** is also known as DORA **12** in reference 5a.

[7] The reduction of bioactivation potential is a generally well accepted de-risking strategy in drug development. For recent reviews, see: a) Stachulski, A. V.; Baillie, T. A.; Park, B. K.; Obach, R. S.; Dalvie, D. K.; Williams, D. P.; Srivastava, A.; Regan, S. L.; Antoine, D. J.; Goldring, C. E. P; Chia, A. J. L.; Kitteringham, N. R.; Randle, L. E.; Callan, H.; Castrejon, L.; Farrell, J.; Naisbitt, D. J.; Lennard, M. S. *Medicinal Res. Rev.* **2013**, *33*, 985-1080; b) Stepan, A. F.; Walker, D. P.; Bauman, J.; Price, D. A.; Baillie, T. A.; Kalgutkar, A. S.; Aleo, M. D. *Chem. Res. Toxicol.* **2011**, *24*, 1345-1410.

[8] Whitman, D. B.; Cox, C. D.; Breslin, M. J.; Brashear, K. M.; Schreier, J. D.; Bogusky, M. J.; Bednar, R. A.; Lemaire, W.; Bruno, J. G.; Hartman, G. D.; Reiss, D. R.; Harrell, C. M.; Kraus, R. L.; Li, Y.; Garson, S. L.; Doran, S. M.; Preuksaritanont, T.; Li, C.; Winrow, C. J.; Koblan, K. S.; Renger, J. J.; Coleman, P. J. *ChemMedChem* **2009**, *4*, 1069 - 1074.

[9] Marugan, J. J.; Zheng, W.; Motabar, O.; Southall, N.; Goldin, E.; Westbroek, W.; Stubblefield, B. K.; Sidransky, E.; Aungst, R. A.; Lea, W. A.; Simeonov, A.; Leister, W.; Austin, C. P. *J. Med. Chem.* **2011**, *54*, 1033.

[10] Kath, J. C.; Richter, D. T.; Luzzio, M. J. Selective synthesis of CF_3-substituted pyrimidines, WO 2005023780.

[11] For additional synthetic details regarding the compounds in this manuscript, see: Bergman, J. M.; Breslin, M. J.; Coleman, P. J.; Cox, C. D.; Mercer, S. P.; Roecker, A. J. Substituted diazepan compounds as orexin receptor antagonists, WO 2008069997.

[12] The lipophilic surface area for DORA **1** is 350 $Å^2$. The isosteric designs represent less than a 10% deviation from the lead compound.

[13] For the details of these in vitro assays, see reference 5a.

[14] For the details of the microsomal GSH trapping assay, see reference 5a.

[15] Pgp and permeability were assayed as described in: (a) Hochman, J. H.; Yamazaki, M.; Ohe, T.; Lin, J. H. *Curr. Drug Metab.* **2002**, *3*, 257-273; (b) Lin, J. H.; Yamazaki, M. *Drug Metab. Rev.* **2003**, *35*, 417-454.

[16] For the details of rat and mouse sleep studies, please see reference 5b.

[17] For the details of the humanized rat occupancy assay, see reference 5a.

[18] (a) Roecker, A. J.; Mercer, S. P.; Schreier, J. D.; Cox, C. D.; Fraley, M. E.; Steen, J. T.; Lemaire, W.; Bruno, J. G.; Harrell, C. M.; Garson, S. L.; Gotter, A. L.; Fox, S. V.; Stevens, J.; Tannenbaum, P. L.; Prueksaritanont, T.; Cabalu, T. D.; Cui, D.; Stellabott, J.; Hartman, G. D.; Young, S. D.; Winrow, C. J.; Renger, J. J.; Coleman, P. J. *ChemMedChem* **2014**, *9*, 312-322; (b) Mercer, S. P.; Roecker, A. J.; Garson, S. L.; Reiss, D. R.; Harrell, C. M.; Murphy, K. L.; Bruno, J. G.; Bednar, R. A.; Lemaire, W.; Cui, D.; Cabalu, T. D.; Tang, C.; Prueksaritanont, T.; Hartman, G. D.; Young, S. D.; Winrow, C. J.; Renger, J. J.; Coleman, P. J. *Bioorg. Med. Chem. Lett.* **2013** *23*, 6620-6624; (c) Roecker, A. J.; Reger, T. S.; Mattern, M. C.; Mercer, S. P.; Bergman, J. M.; Schreier, J. D.; Cube, R. V.; Cox, C. D.; Li, D.; Lemaire, W.; Bruno, J. G.; Harrell, C. M.; Garson, S. L.; Gotter, A. L.; Fox, S. V.; Stevens, J.; Tannenbaum, P. L.; Prueksaritanont, T.; Cabalu, T. D.; Cui, D.; Stellabott, J.; Hartman, G. D.; Young, S. D.; Winrow, C. J.; Renger, J. J.; Coleman, P. J. *Bioorg. Med. Chem. Lett.* **2014**, *24*, 4884-4890; (d) Lebold, T. P.; Bonaventure, P.; Shireman, B. T. *Bioorg. Med. Chem. Lett.* **2013**, *23*, 4761-4769; (e) Fujimoto, T.; Kunitomo, J.; Tomata, Y.; Nishiyama, K.; Nakashima, M.; Hirozane, M.; Yohikubo, S.-I.; Hirai, K.; Marui, S. *Bioorg. Med. Chem. Lett.* **2011**, *21*,

6414-6416; (f) T. Fujimoto, Y. Tomata, J. Kunitomo, M. Hirozane, S. Marui, *Bioorg. Med. Chem. Lett.* **2011**, *21*, 6409-6413; (g) Betschart, C.; Hintermann, S.; Behnke, D.; Cotesta, S.; Fendt, M.; Gee, C. E.; Jacobson, L. H.; Laue, G.; Ofner, S.; Chaudhari, V.; Badiger, S.; Pandit, C.; Wagner, J.; Hoyer, D. *J. Med. Chem.* **2013**, *56*, 7590-7607.

[19] The 2-methoxypyrimidine variant of 2-SORA **15** was synthesized and demonstrated an OX_2R IC_{50} of 245 nM and selectivity over OX_1R of 7-fold. This further highlights the stringent SAR around orexin subtype selectivity.

[20] While mouse plasma protein binding is unavailable for 2-SORA **19**, it is anticipated that the free concentration at C_{max} is well below the OX_1R IC_{50} in this experiment suggesting low OX_1R blockade during this mouse sleep study.

[21] For medicinal chemistry details concerning MK-1064 and MK-3697, see references 15a and 15c.